NASA TM X-375

NASA TM X-375

TECHNICAL MEMORANDUM

X-375

SUPERSONIC AERODYNAMIC PERFORMANCE AND STATIC-STABILITY CHARACTERISTICS OF TWO BLUNT-NOSED, MODIFIED 13° HALF-CONE CONFIGURATIONS

By John V. Rakich

Ames Research Center
Moffett Field, Calif.

NATIONAL AERONAUTICS AND SPACE ADMINISTRATION
WASHINGTON
September 1960

[redacted]

NATIONAL AERONAUTICS AND SPACE ADMINISTRATION

TECHNICAL MEMORANDUM X-375

SUPERSONIC AERODYNAMIC PERFORMANCE AND STATIC-STABILITY CHARACTERISTICS OF TWO BLUNT-NOSED, MODIFIED 13° HALF-CONE CONFIGURATIONS*

By John V. Rakich

SUMMARY

A preliminary investigation has been made of the performance and stability of a blunt-nosed half-cone configuration (13° semiapex angle) suitable for entry from satellite orbit. Maneuverability requirements, and thus the lift-drag ratio, were fixed by the desirability of returning to the launch site after one circumnavigation of the earth. This lateral range capability (in the order of 1200 nautical miles) requires a lift-drag ratio near 1.5 at hypersonic speeds. A maximum stagnation-point radiation-equilibrium temperature of 4000° F, together with the desired lift-drag ratio was used to establish the cone angle and the radius of curvature required for the blunt nose.

Experimental results for the basic (near half-cone) configuration obtained at Mach numbers from 3 to 5 indicate a maximum lift-drag ratio of 1.3 with a trim point near zero lift coefficient. The configuration had static longitudinal, directional, and lateral stability. A modification to the basic configuration resulted in essentially unchanged performance and in a shift of the trim point to a lift coefficient which corresponds approximately with maximum lift-drag ratio. The modification consisted of cutting off a segment of the lower, after part of the half-cone body along a plane parallel with the cone axis.

The measured and estimated aerodynamic characteristics were in good agreement, with the exception of the pitching-moment coefficient and the directional stability.

[redacted] Unclassified

[redacted]

INTRODUCTION

The effects of lift and drag on the trajectory and heating of vehicles entering the earth's atmosphere have been well established theoretically (see, e.g., refs. 1, 2, 3). Specifically it has been found that increasing lift decreases heating rates, while increasing lift-drag ratio decreases decelerations and increases the maneuverability and total heat convected during gliding entry from satellite orbit. Because of these varied effects, the design of a manned, lifting entry vehicle is, in essence, a compromise of maneuverability, physiological, and structural-material requirements. For a specified mission, the design must result in tolerable decelerations and heat loads compatible with material properties.

These considerations were used by Eggers and Wong (ref. 2) in selecting a near half-cone configuration for study as a manned near-earth satellite vehicle. This configuration was designed for high drag as well as high lift, and had a lift-drag ratio of about 0.5 at high speeds. With this lift-drag ratio, the 30° half-cone of reference 2 incurs deceleration well within the range of human tolerance, but the maneuverability is somewhat limited. For example, its lateral range capability during entry is about 200 nautical miles. Since greater maneuverability may be desired, vehicles with maximum lift-drag ratios greater than that of the vehicle of reference 2 are also of interest. Such a vehicle is the subject of the present investigation. In particular, the high-speed aerodynamic characteristics of a configuration similar to (but more slender than) the vehicle of reference 2 are studied theoretically and experimentally at Mach numbers from 3 to 5. The specific shape of the study configuration (viz. nose bluntness and cone angle) is selected so that a full-scale vehicle of reasonable size and weight would have acceptable heating characteristics.

CONFIGURATION

It appears that lateral range is one of the primary factors in setting the aerodynamic performance requirements for a satellite entry vehicle. One use for lateral range is indicated in figure 1(a) where the lateral range required for a unit orbit transfer is shown for various latitudes and orbit inclinations. It may be seen in this figure that for a launching site in the southern extreme of the United States and for a polar orbit at an altitude of 100 miles, a lateral range of 1200 nautical miles is required to enable a vehicle to return to the launching site after one circumnavigation of the earth. It appears then that a lateral range of 1200 nautical miles is a useful and reasonable requirement for a vehicle.

From trajectory studies made using a digital computer, the aerodynamic performance required to obtain a given lateral range was established (ref. 4). The results are shown in figure 1(b) which presents the obtainable lateral range as a function of lift-drag ratio. From these results, it was found that a lateral range of 1200 nautical miles can be obtained during entry from a satellite orbit with a vehicle developing a lift-drag ratio of 1.5. Thus a nominal lift-drag ratio of 1.5 was chosen for the present study. Note, however, that this condition may be relaxed somewhat while a unit orbit transfer capability is maintained for most orbits of interest.

It remains then to select a configuration with a lift-drag ratio of 1.5. While any number of vehicles will meet this requirement, the present study was restricted to simple half-cones similar to that reported in reference 2. In addition, full-scale dimensions were selected so that heating rates and thus maximum surface temperatures could be estimated. In particular, a full-scale base diameter of 10 feet was set so the vehicle would have sufficient size and volume to hold two men. With these conditions, Newtonian impact theory was used to estimate the aerodynamic characteristics and the equilibrium glide condition was used to approximate the trajectories for a series of blunt-nosed half-cones. Lift-drag ratios and maximum stagnation-point radiation-equilibrium temperatures were calculated for ranges of lift coefficients and vehicle weights. Based on the results of these calculations, a semiapex angle of 13° and a full-scale nose radius of 1.5 feet were selected. The resultant configuration, including a canopy, is shown in figure 2 along with its estimated full-scale dimensions. For this vehicle, figure 3 shows the variations, with lift coefficient, of the predicted lift-drag ratio and maximum stagnation-point radiation-equilibrium temperature. Note that the temperatures shown in this figure are for maneuvering entry; that is, the vehicle is assumed to be in a 45° roll attitude since this is the attitude which gives maximum lateral range for low lift-drag ratios. In the present study, it is assumed that radiation-equilibrium temperatures up to 4000° F are permissible since foamed ceramics capable of withstanding this temperature are under development (see refs. 5 and 6). It may be seen that, for an emissivity of 0.8, a 6000-pound vehicle could operate near maximum lift-drag ratio without the stagnation-point radiation-equilibrium temperature exceeding 4000° F. With a heavier vehicle, allowable temperatures could be maintained by flying at increased lift coefficient during peak heating conditions. The radiation-equilibrium temperature distributions for the underside of the configuration, computed by the method of reference 7, are shown in figure 4. It can be seen in this figure that the temperature markedly decreases downstream from the stagnation point, and that, near the base, it approaches one-half of the stagnation value. Thus if some cooling technique can be employed in a small region near the nose, the restrictions imposed by heating can be greatly relaxed.

[redacted]

EXPERIMENT AND TEST APPARATUS

An experimental program was conducted to determine the high-speed aerodynamic performance and static stability characteristics of the configuration selected, and to determine the adequacy of the impact-theory calculations used in this preliminary design. Tests were conducted in the Ames 10- by 14-Inch Supersonic Wind Tunnel (ref. 8) at Mach numbers of 3, 4, and 5 and at angles of attack up to 32°. Lateral stability characteristics were obtained at several angles of attack by testing at angles of sideslip up to 4°. Aerodynamic forces and moments were measured with a six-component strain-gage balance. The base pressures were determined with a strain-gage-type pressure cell. Wind-tunnel test conditions are shown in table I; note that the test Reynolds number was reduced for operation at M = 3 when the model angle of attack was greater than 17°.

Sketches of the wind-tunnel models are shown in figure 5. Model 1 consists of a 13° half-cone, blunted with a quarter-sphere nose, and topped with a wedge section on the flat portion of the half-cone. Model 1a is the modification of model 1 obtained by cutting the underside of the model near the base along a plane parallel to the cone axis and perpendicular to the vertical plane of symmetry of the model. Model 1a also includes a canopy which is a segment of a sphere.

All aerodynamic coefficients are referred to the model plan area; pitching-moment coefficient is referred to model length, and roll and yawing-moment coefficients to the model base span. The base pressure force (i.e., base drag) is included in the aerodynamic coefficients. It is believed that sting interference effects were small since the sting area is less than 20 percent of the base area. Lift, drag, and pitching-moment coefficients are presented with respect to wind axes and the side-force, yawing-moment, and rolling-moment coefficients with respect to body axes. The angle of attack is defined with respect to the cone axis.

Accuracy of the test results is primarily influenced by uncertainties in the measurements of forces and moments, in the determination of stream dynamic pressure, and in obtaining the angle of attack. Of these, the uncertainties in the force and moment measurements are the most prominent factors. The estimated uncertainties in the various parameters are shown in the table below.

α	±0.2°	C_m	±0.003
M	±0.10	C_{Y_β}	±0.050
C_L	±0.005	C_{n_β}	±0.005
C_D	±0.005	C_{l_β}	±0.005
L/D	±0.05		

[redacted]

RESULTS AND DISCUSSION

The experimental results obtained in the present investigation are shown in figures 6, 7, and 8 together with estimated aerodynamic characteristics. Typical base-pressure coefficients are tabulated in table II. For the estimated characteristics shown in the figures, Newtonian impact theory ($C_p = 2 \sin^2\delta$)[1] was applied to the nose and conical portions of the configurations. To estimate the pressure coefficient on the flat upper surface and on the flat surface at the bottom rear of the modified configuration, Prandtl-Meyer expansion was used when these surfaces were shielded from the wind. When they were not shielded, linear theory was used up to the flow deflection where the pressure coefficient obtained with impact theory exceeded that obtained by linear theory. For greater flow deflections, impact theory was used for the flat surfaces also. Base drag was approximated with a base pressure coefficient of $C_{p_b} = -1/M^2$. This approximation seems a reasonable one as shown in table II. Finally, a friction-drag coefficient of 0.006 was assumed.

As may be seen in figure 6, the methods just described provide good estimates of the experimental results for C_L and L/D. Both the theoretical and the experimental results shown in this figure indicate a maximum lift-drag ratio of about 1.3 for the configuration at all test Mach numbers. As previously noted, these results include the base drag. If the base drag were nearly zero, as might be more representative of results for higher Mach numbers, the maximum lift-drag ratio would be very nearly the desired value of 1.5. In addition, a small discontinuity in the data is observed at 18° angle of attack in figure 6(a). Although the test Reynolds number changed at this angle, it is believed that the discontinuity is primarily due to experimental scatter.

The longitudinal stability is predicted reasonably well, whereas the theoretical estimate for the pitching moment is not in good agreement with experimental results. The reason for this poor agreement is apparently that the pressures on the upper surface near the nose of the body are underestimated by the methods described. With some approximations, the pressures on the upper surface were estimated with blast-wave theory (see, e.g., ref. 9). The resultant estimate of the increment in pitching-moment coefficient at zero angle of attack was about -0.01. This increment, if applied to the theory shown in figure 6, would improve agreement with experiment at the higher Mach numbers, at which blast-wave theory is applicable. Model 1 trims near zero-lift coefficient rather than near maximum lift-drag ratio as estimated. To correct this situation, this configuration was modified, as previously indicated, to shift the trim point to a higher lift coefficient. Model 1a (fig. 5) resulted from this modification. The longitudinal characteristics of the

---

[1]See appendix for symbols.

modified configuration with and without a canopy are shown in figure 7. The modified configuration trims at a lift coefficient which coincides approximately with maximum lift-drag ratio. Its longitudinal stability is about the same as that of the basic configuration. The maximum lift-drag ratio is about 1.4 without the canopy; however, addition of the canopy reduces the maximum lift-drag ratio by about 0.1 to about 1.3, approximately the value for the basic configuration. The effect of the canopy on the moment coefficients is within the accuracy of the experimental results.

The directional and lateral-stability characteristics of the basic configuration are shown in figure 8. With the exception of the directional stability, C_{n_β}, the method previously described yields accurate estimates of these characteristics; directional stability is somewhat underestimated. The results show the basic configuration to be directionally stable; however, based on conventional aircraft standards, the dihedral effect is somewhat larger than might be desired.

CONCLUDING REMARKS

The aerodynamic characteristics of a blunt-nosed half-cone configuration were investigated theoretically and experimentally at Mach numbers from 3 to 5. The configuration was formed from a cone with a semiapex angle of 13°; its nose radius was 0.15 base diameter. The configuration was selected to have a maximum lift-drag ratio of 1.5 at hypersonic speeds while experiencing maximum stagnation point radiation-equilibrium temperatures less than 4000° F during entry from a satellite orbit. With this lift-drag ratio, the configuration should possess a unit orbit transfer capability (lateral range of about 1200 nautical miles).

The experimental results indicate that the configuration had static longitudinal, directional, and lateral stability. The maximum lift-drag ratio (including the effect of base drag) at the test Mach numbers was about 1.3, but the configuration trimmed at zero lift coefficient. A modification to the basic configuration resulted in essentially unchanged performance and in a shift of the trim point to a lift coefficient which corresponded approximately with maximum lift-drag ratio. The modification consisted of removal of a segment of the lower after part of the conical surface.

Estimated aerodynamic characteristics were in good agreement with experimental results, with the exception of pitching-moment coefficient and directional stability.

Ames Research Center
National Aeronautics and Space Administration
Moffett Field, Calif., April 25, 1960

APPENDIX

NOTATION

b	maximum span (at base)
C_D	drag coefficient, $\frac{\text{drag}}{q_\infty S}$
C_l	rolling-moment coefficient, $\frac{\text{rolling moment}}{q_\infty S b}$
C_L	lift coefficient, $\frac{\text{lift force}}{q_\infty S}$
C_m	pitching-moment coefficient, $\frac{\text{pitching moment}}{q_\infty S l}$
C_n	yawing-moment coefficient, $\frac{\text{yawing moment}}{q_\infty S b}$
C_P	pressure coefficient, $\frac{p - p_\infty}{q_\infty}$
C_Y	side-force coefficient, $\frac{\text{side force}}{q_\infty S}$
l	total length (parallel to cone axis)
$\frac{L}{D}$	lift-drag ratio
M	Mach number
p	pressure
q	dynamic pressure
Re	Reynolds number
S	plan area
T	temperature
x	distance from nose parallel to cone axis
α	angle of attack (measured from cone axis)
β	angle of sideslip (measured from cone axis)
δ	local slope of surface with respect to wind

θ angle from vertical plane of symmetry

Subscripts

b base

s stagnation point

t total conditions

β derivative with respect to β, evaluated at $\beta = 0$, per radian

∞ free-stream conditions

[redacted]

REFERENCES

1. Eggers, Alfred J., Jr., Allen H. Julian, and Neice, Stanford E.: A Comparative Analysis of the Performance of Long-Range Hypervelocity Vehicles. NACA TN 4046, 1957.

2. Eggers, Alfred J., Jr. and Wong, Thomas J.: Re-entry and Recovery of Near-Earth Satellites, With Particular Attention to a Manned Vehicle. NASA MEMO 10-2-58A, 1958.

3. Eggers, Alfred J., Jr.: The Possibility of a Safe Landing. Space Technology, Howard Seifert, ed., John Wiley and Sons, Inc., 1959, pp. 13-01 - 13-53.

4. Slye, Robert E.: An Analytical Method for Studying the Lateral Motions of Atmosphere Entry Vehicles. NASA TN D 325, 1960.

5. Jordon, P. F., and Barrett, W. F.: Some Nose Cap Studies for a Manned Re-entry Glider. Space Flight Division, The Martin Co. (Baltimore) (Paper presented at the Fourth STL Symposium on Ballistic Missile and Space Technology, 24-27 Aug. 1959 at UCLA).

6. Strauss, Eric L.: Development of Resin-Impregnated Porous Ceramics. Martin RM-51, Sept. 1959.

7. Lees, L.: Laminar Heat Transfer Over Blunt-Nosed Bodies at Hypersonic Flight Speeds. Jet Propulsion, vol. 26, no. 4, April 1956, pp. 259-269.

8. Eggers, A. J., Jr., and Nothwang, George J.: The Ames 10- by 14-Inch Supersonic Wind Tunnel. NACA TN 3095, 1954.

9. Lees, Lester, and Kubota, Toshi: Inviscid Hypersonic Flow Over Blunt-Nosed Slender Bodies. Jour. Aero. Sci., vol. 24, no. 3, March 1957, pp. 195-202 (also CIT pub. 410).

[redacted]

TABLE I.- WIND-TUNNEL TEST CONDITIONS

M	p_t, psia	T_t, °F	Re/l, ft^{-1}
3	20[1] ~ 30	50	$3.4^{1} \sim 5.1 \times 10^6$
4	85	50	8.9×10^6
5	87	200	3.8×10^6

[1]At angles of attack greater than 17°.

TABLE II.- TYPICAL BASE PRESSURE COEFFICIENTS

M	α, deg	C_{p_b}	$-1/M^2$
3	-4.0	-0.110	-0.111
	0	-.108	
	4.2	-.111	
	8.3	-.115	
	12.4	-.120	
4	-4.0	-.067	-.063
	0	-.066	
	4.2	-.069	
	8.3	-.072	
	12.5	-.073	
5	-4.0	-.035	-.040
	0	-.035	
	4.1	-.038	
	8.1	-.041	
	12.2	-.042	

[redacted]

[redacted]

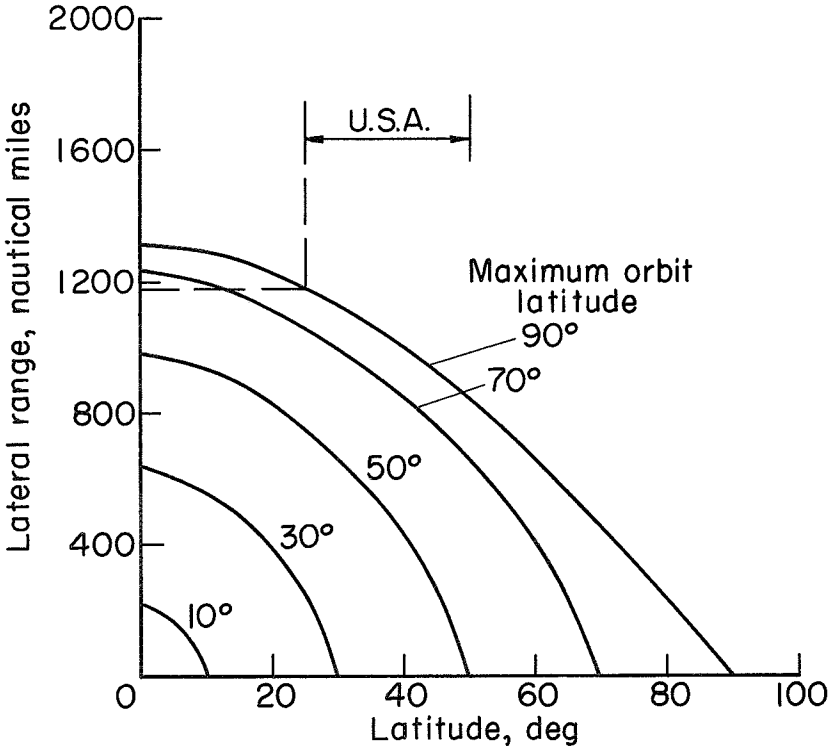

(a) Range requirement for unit orbit transfer (100 mile circular orbit)

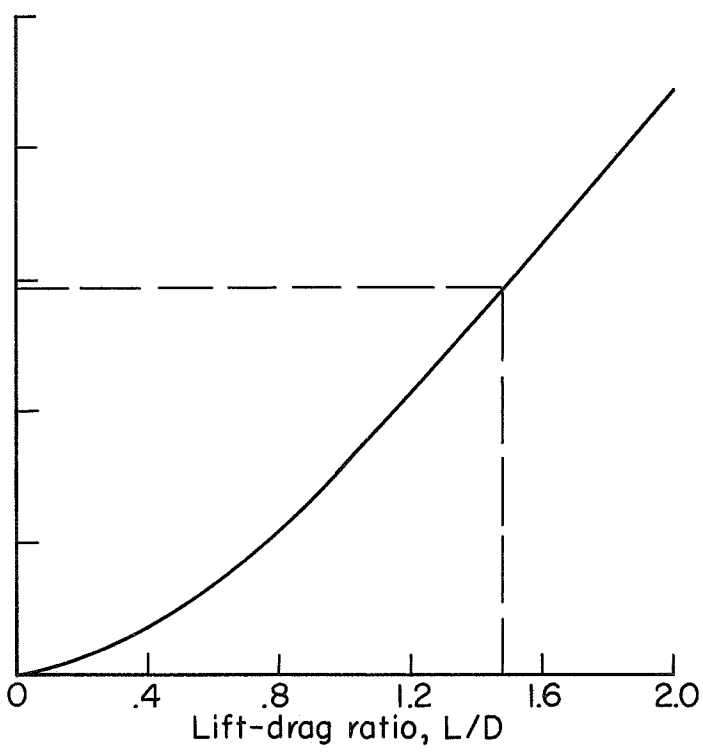

(b) Aerodynamic performance requirement

Figure 1.- Maneuverability requirement.

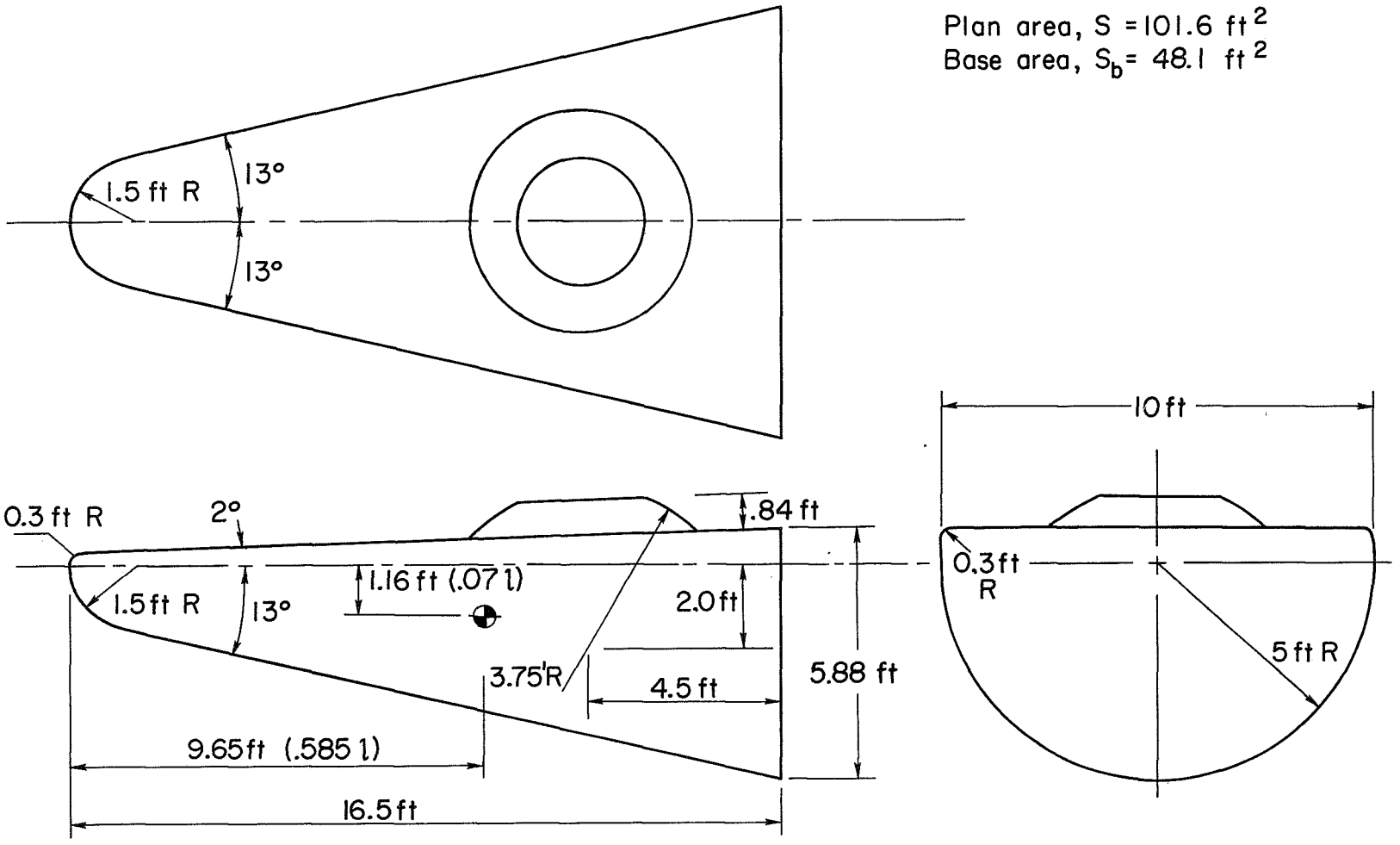

Figure 2.- Preliminary study configuration (full size dimensions).

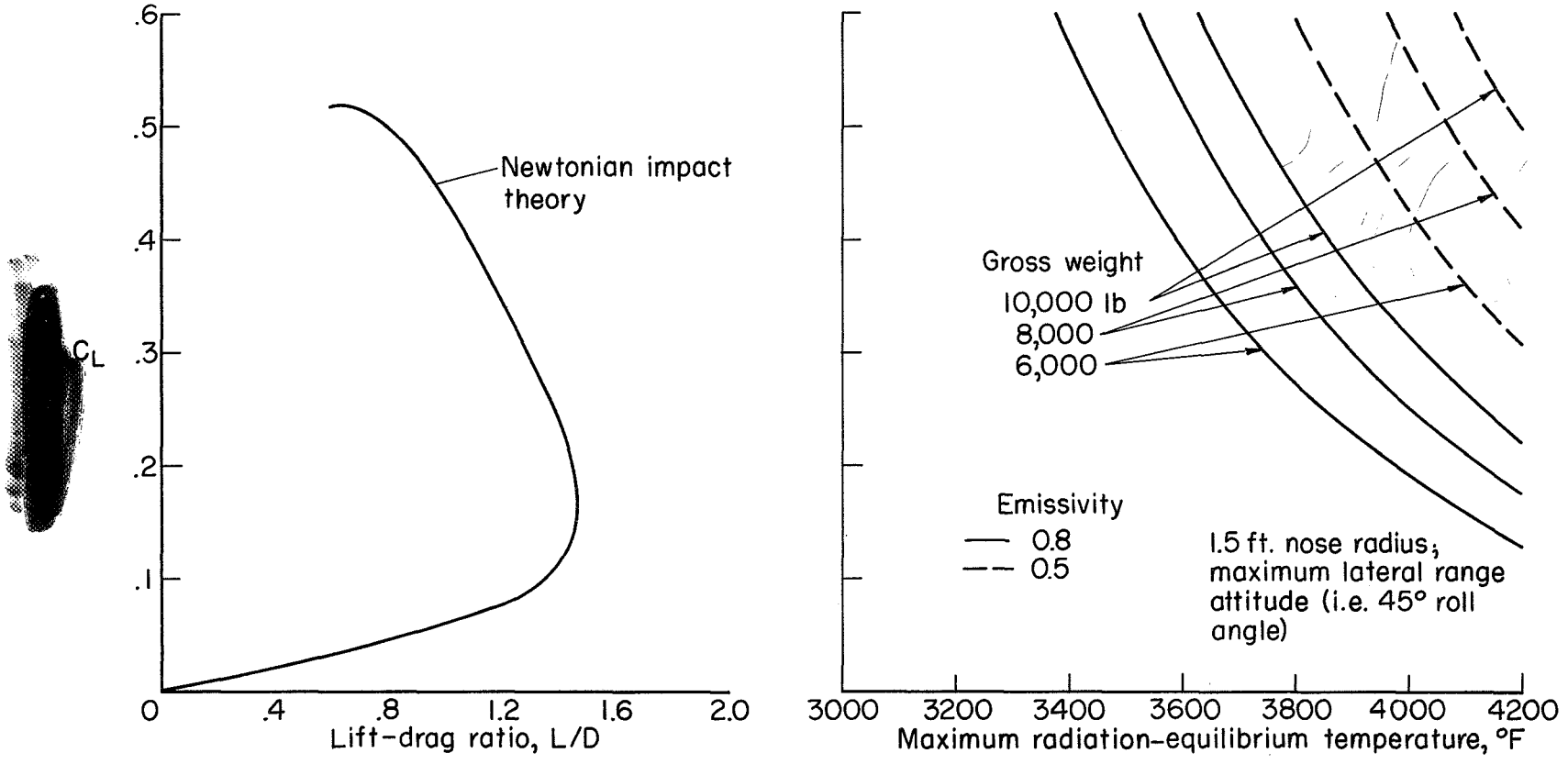

Figure 3.- Predicted heating and aerodynamic performance characteristics.

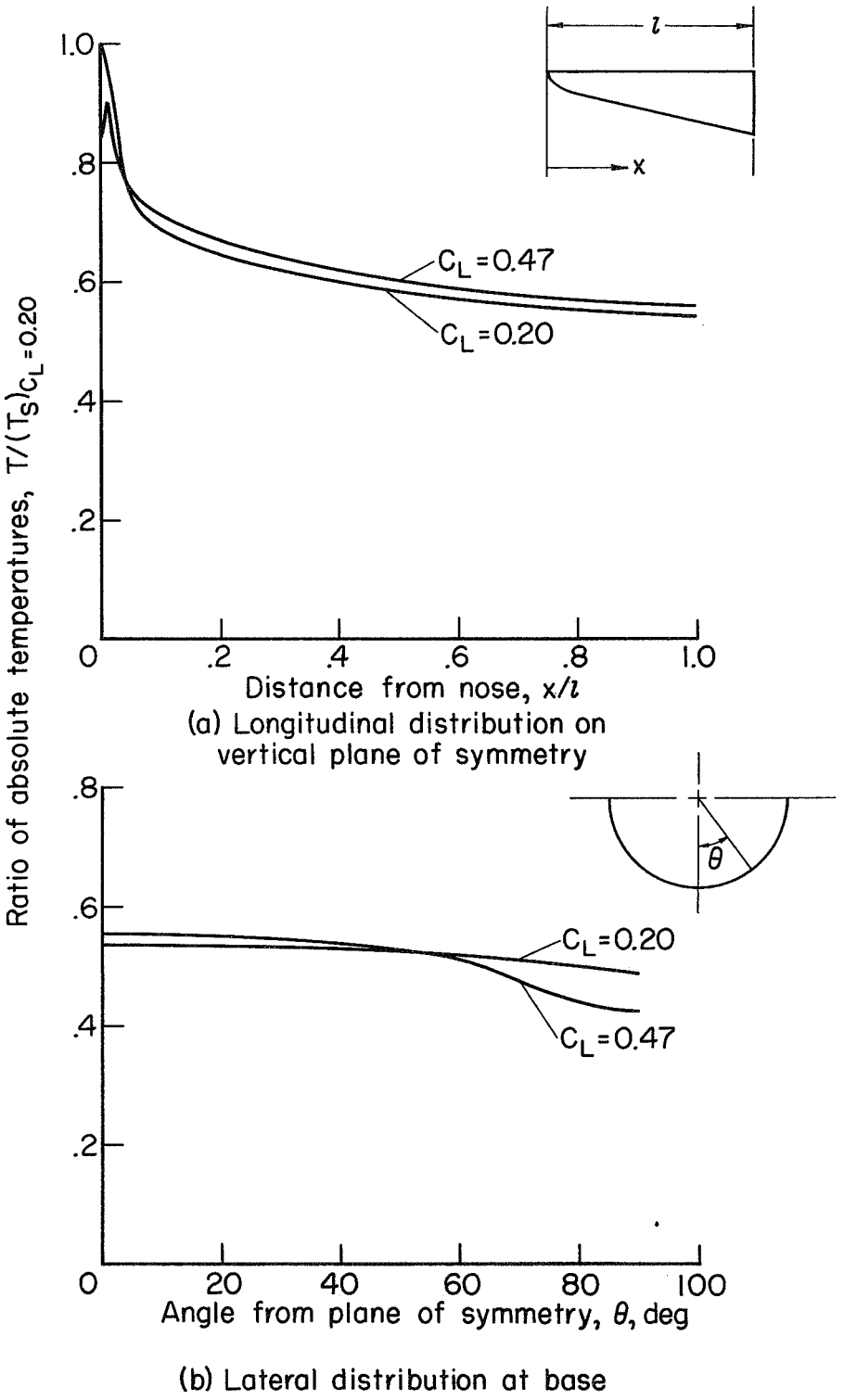

Figure 4.- Temperature distribution on undersurface of study configuration.

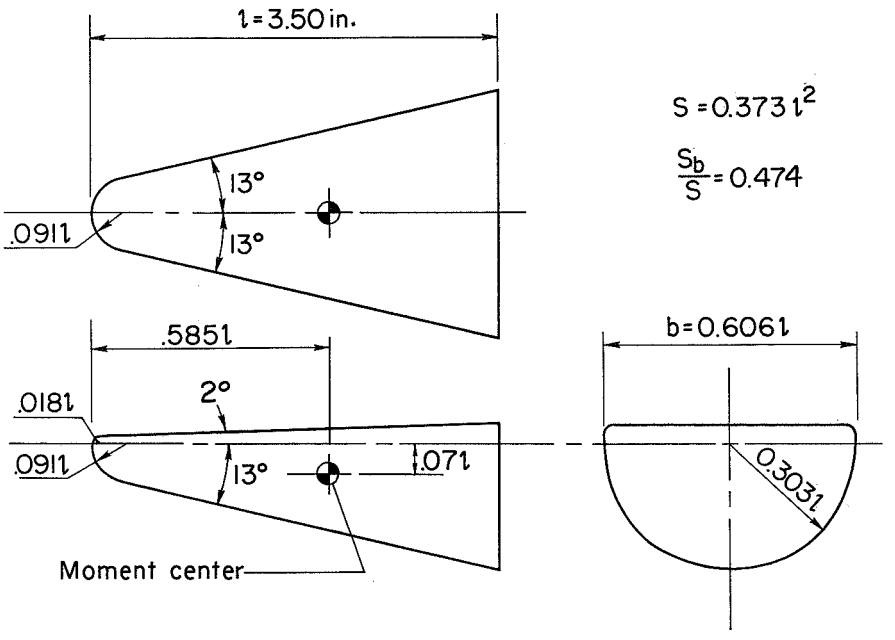

(a) - Model I

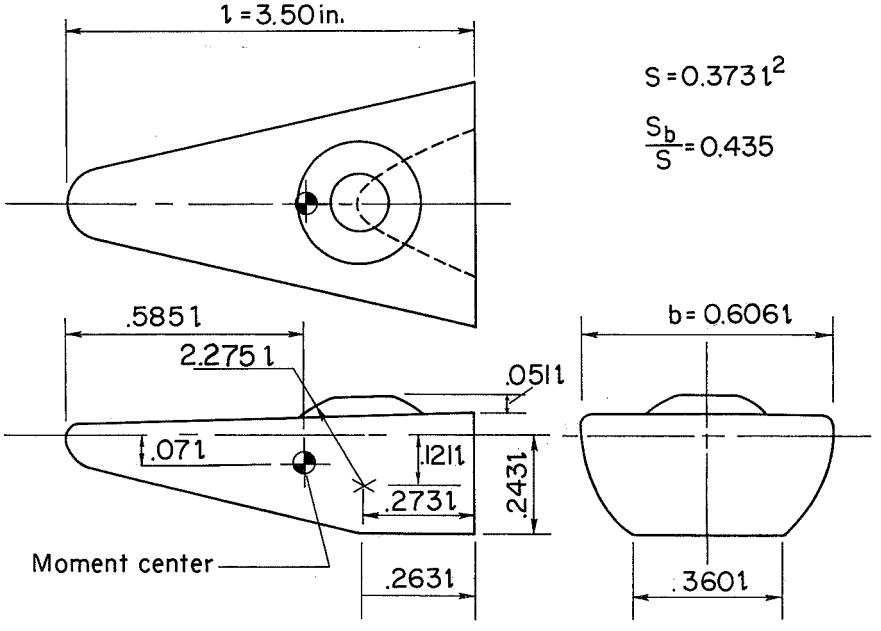

(b) - Model Ia

Figure 5.- Wind tunnel models.

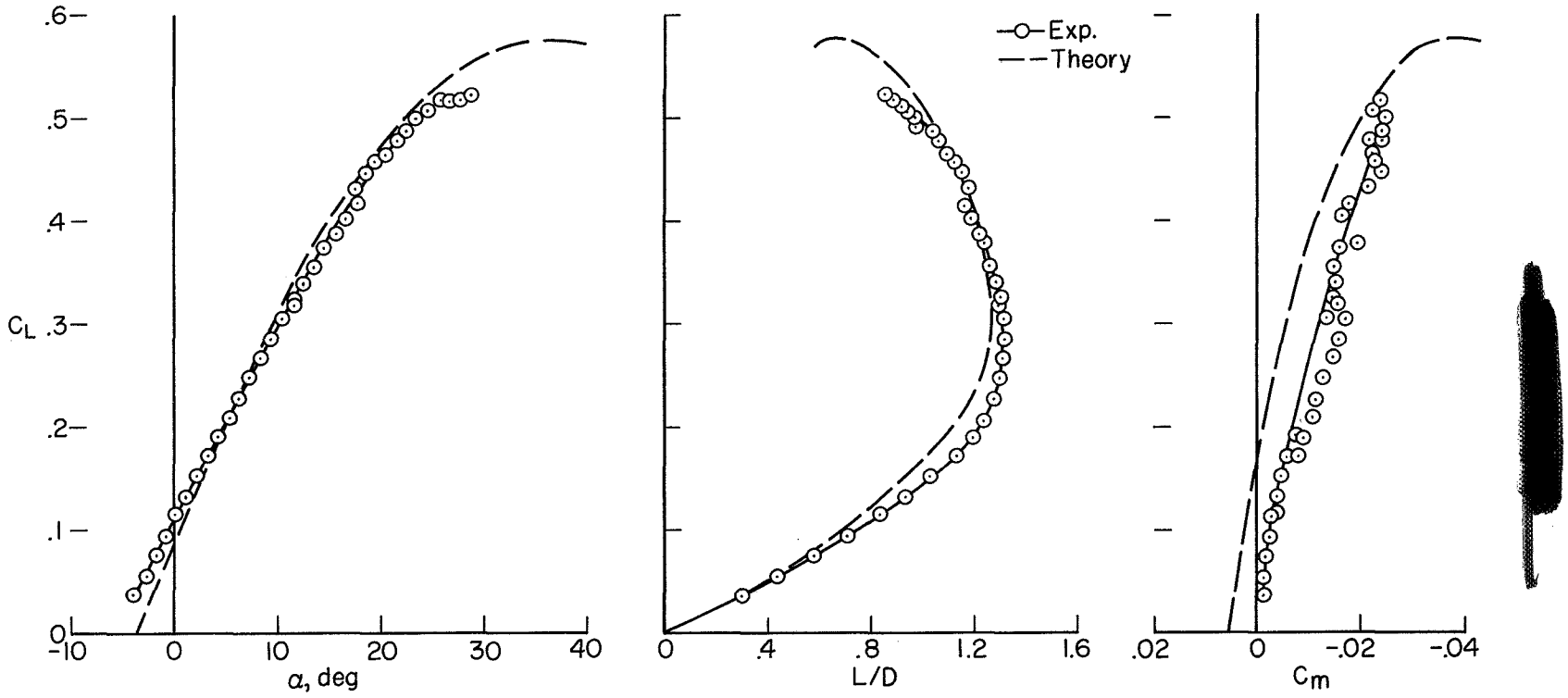

(a) M = 3.0

Figure 6.- Longitudinal aerodynamic characteristics of model 1.

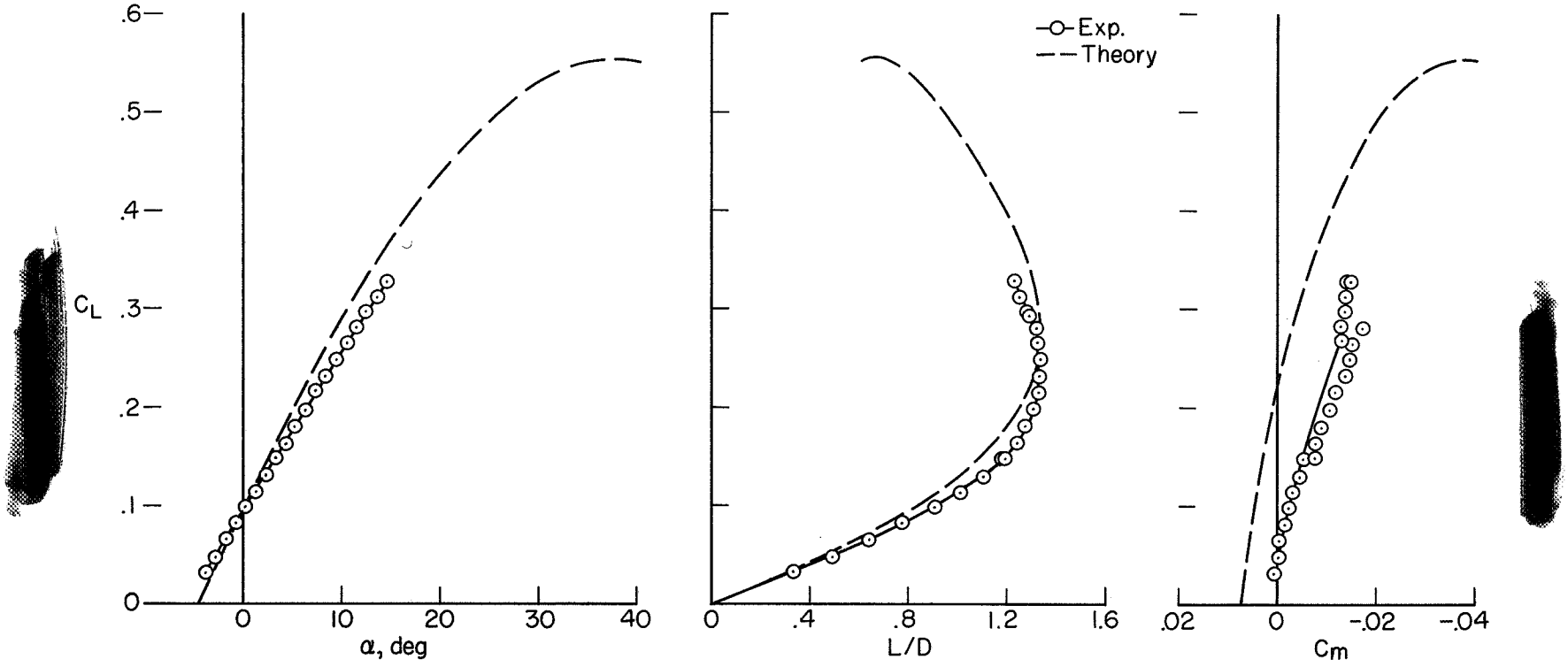

(b) M = 4.0

Figure 6.- Continued.

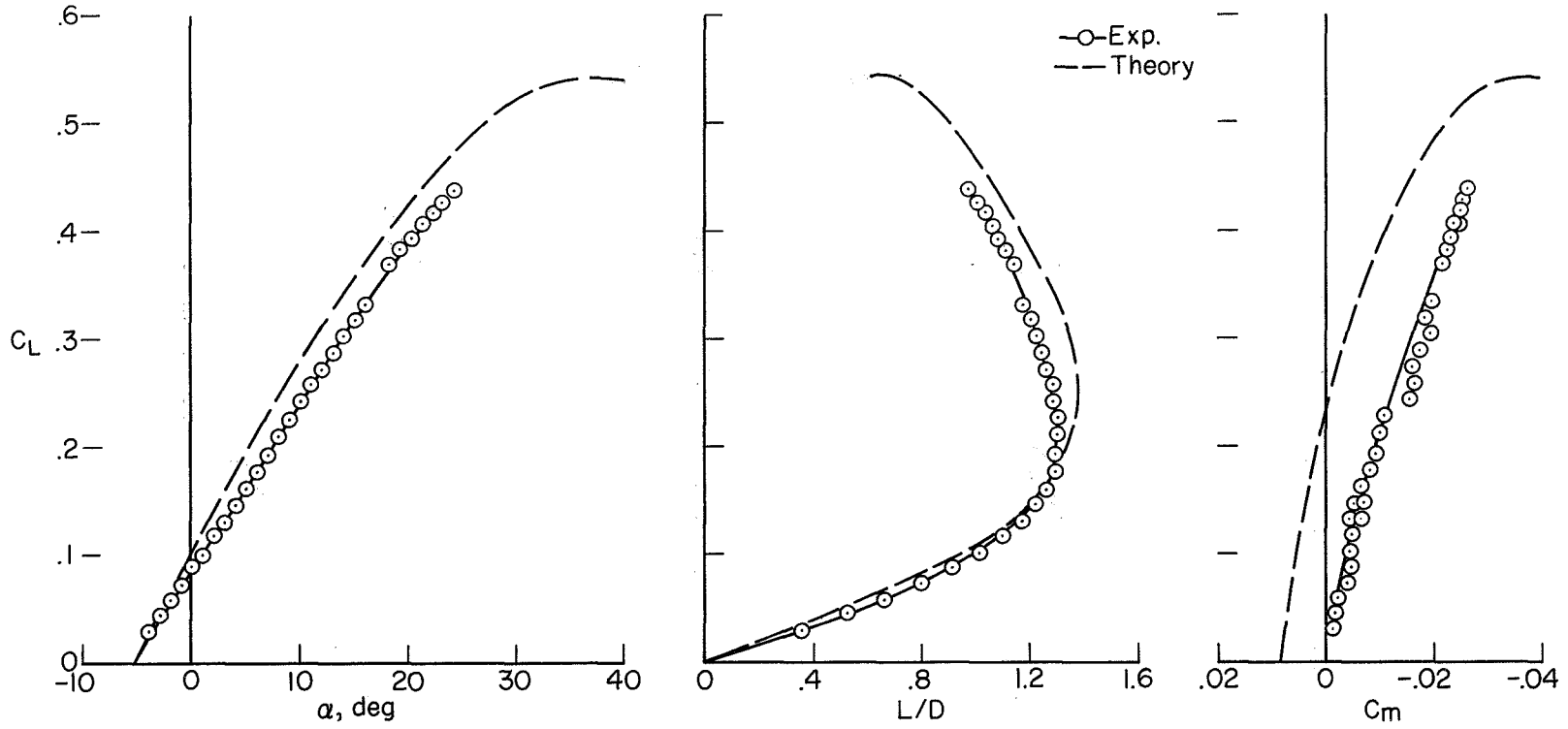

(c) M = 5.0

Figure 6.- Concluded.

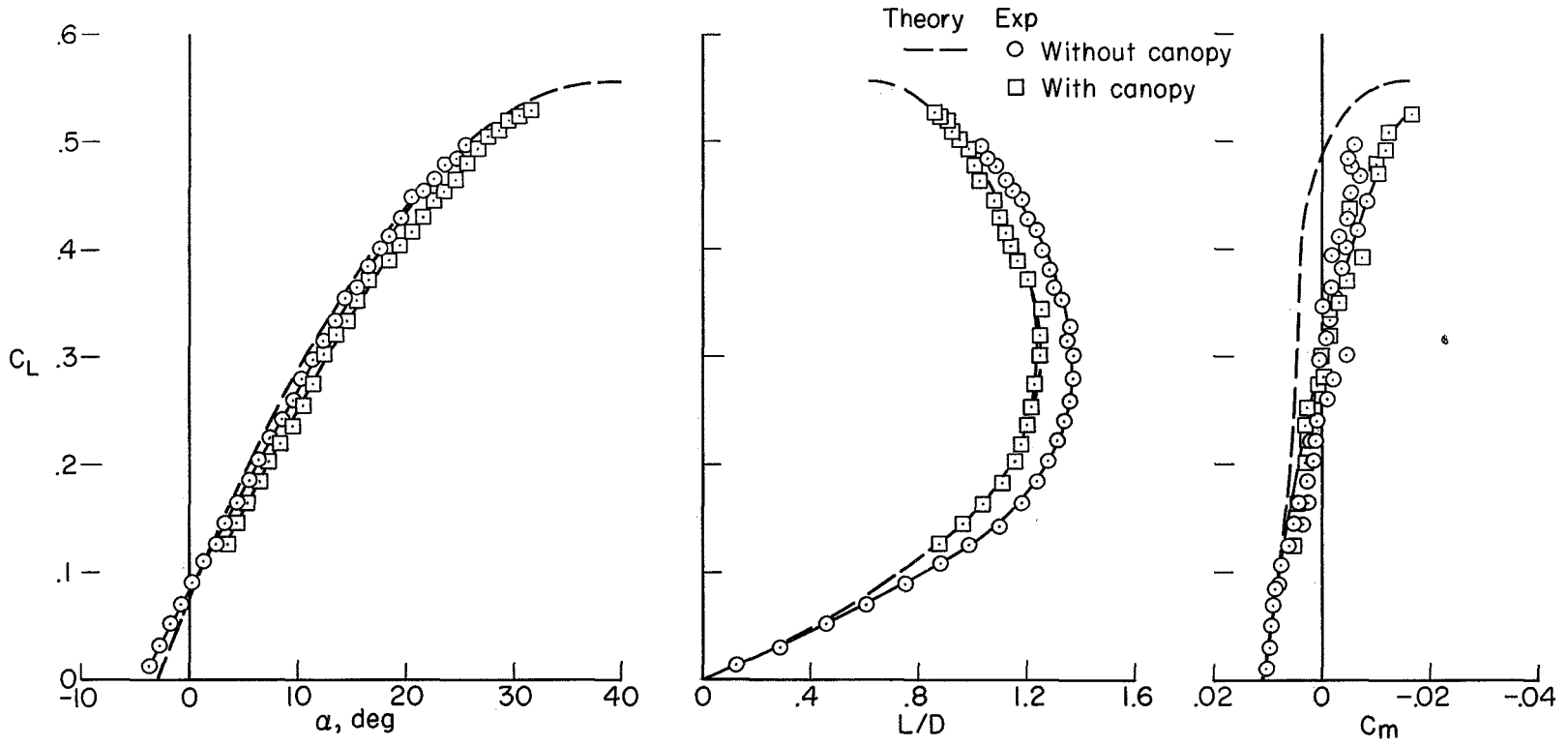

(a) M = 3.0

Figure 7.- Longitudinal aerodynamic characteristics of model 1a.

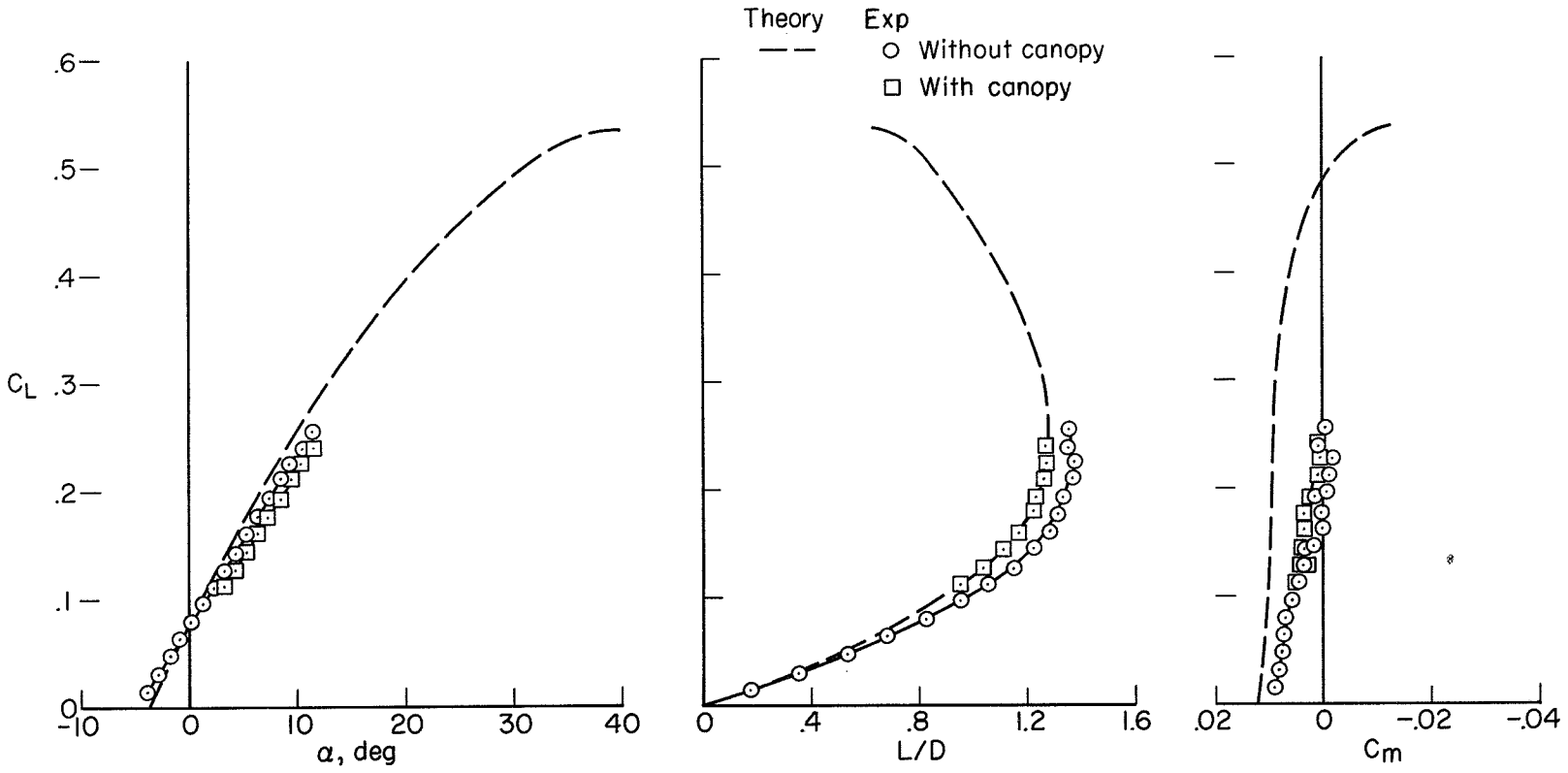

(b) M = 4.0

Figure 7.- Continued.

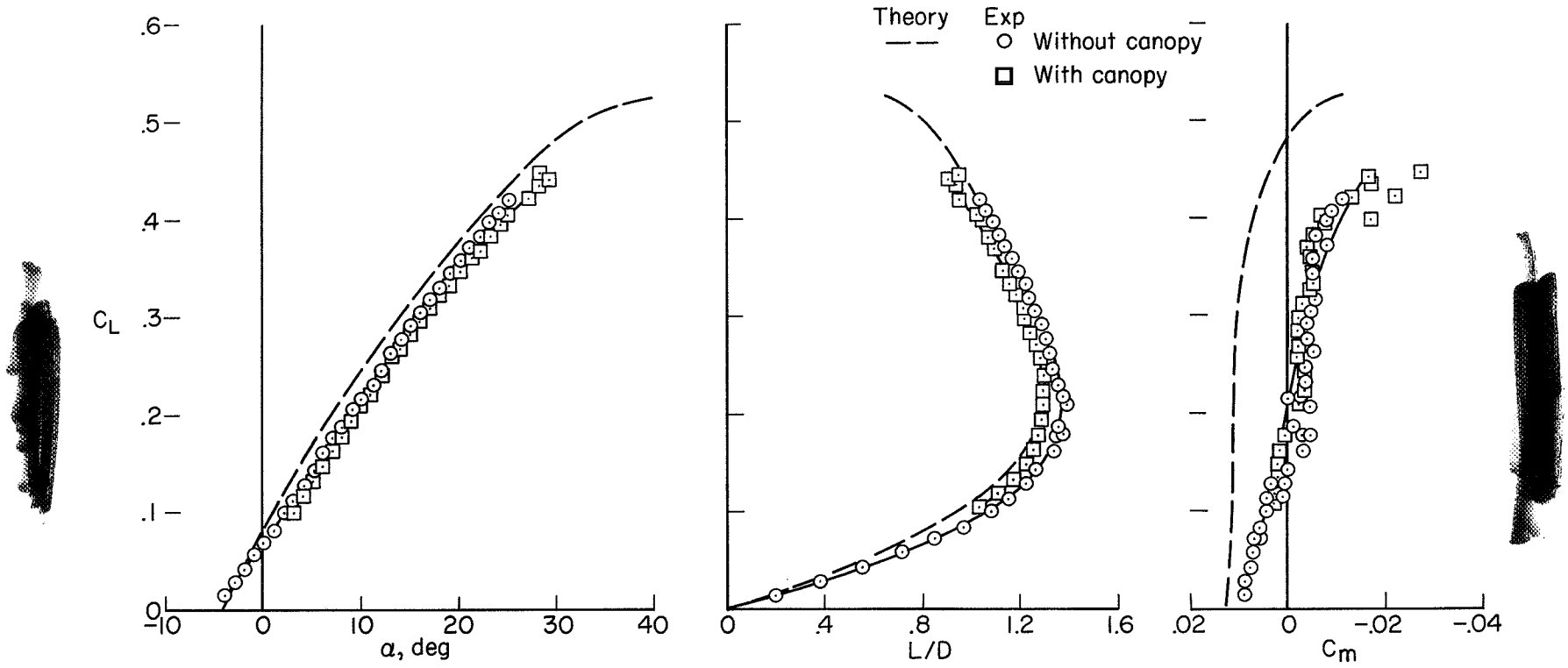

(c) M = 5.0

Figure 7.- Concluded.

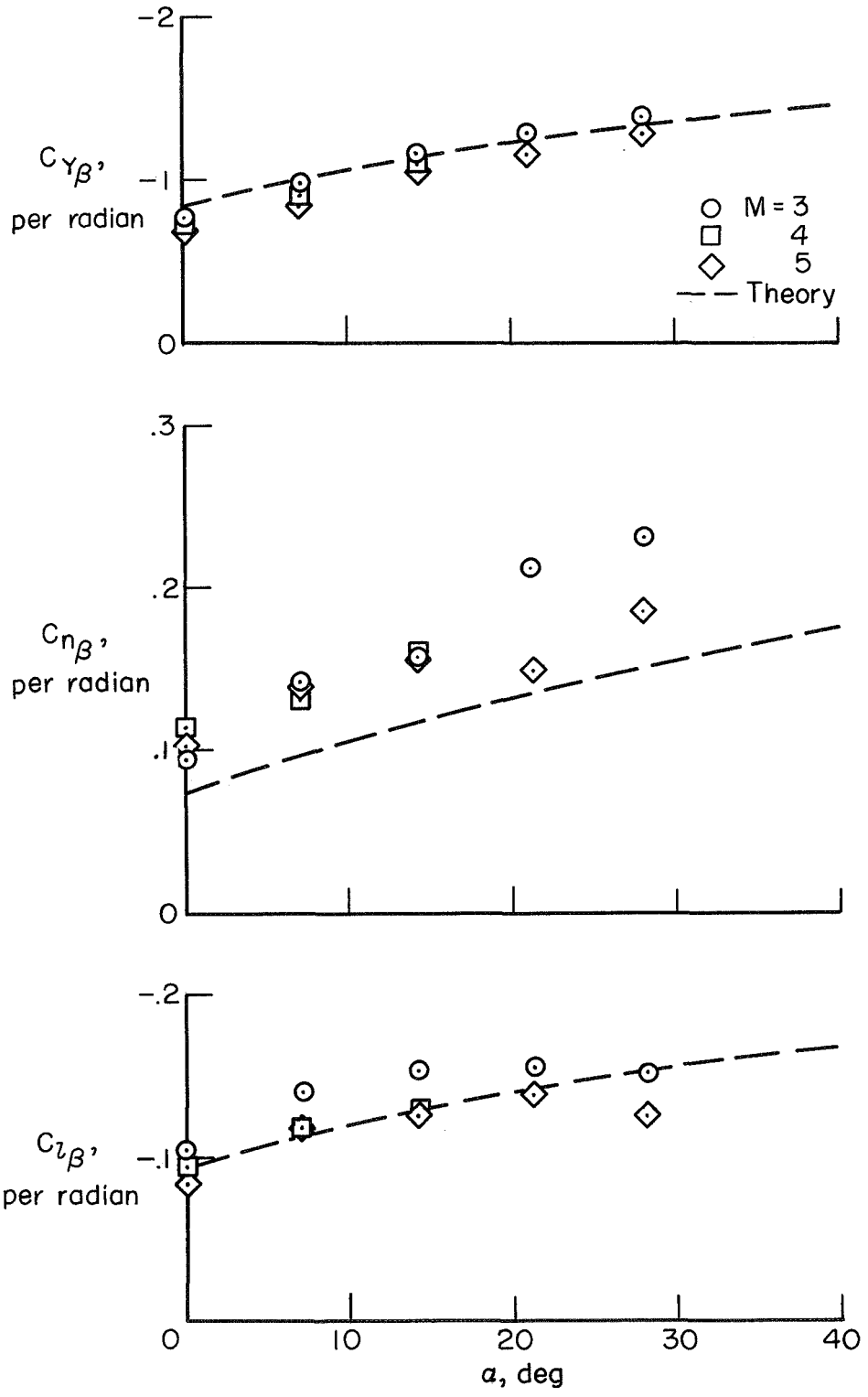

Figure 8.- Lateral aerodynamic characteristics of model 1.